Near-Field Radiative Energy Conversion Devices

Zhuomin Zhang, Ph.D.
J. Erskine Love, Jr. Professor
George W. Woodruff School of Mechanical Engineering
Georgia Institute of Technology, Atlanta, Georgia

Presented at **KITP, UC Santa Barbara**
Emerging Regimes and Implications of Quantum and Thermal Fluctuational Electrodynamics, June 20-August 4, 2022
June 21, 2022

Outline

- Introduction
- Thermophotovoltaic and other photonic energy conversion devices
- Photon chemical potential
- Device analysis and modeling
- Summary and open questions
- Acknowledgments

Thermal Radiation: Far Field vs. Near Field

$d \gg \lambda_{\mathrm{th}}$

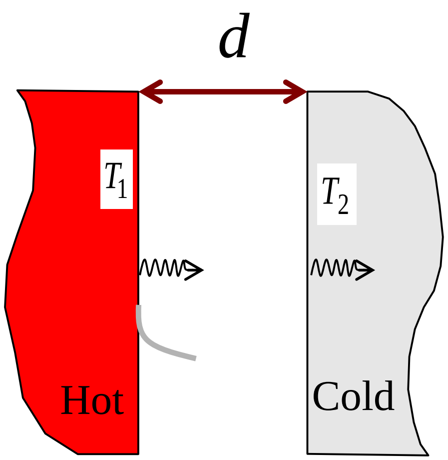

The Stefan-Boltzmann law (1885), the upper limit for propagating modes:

$$q_{\mathrm{BB}} = \sigma\left(T_1^4 - T_2^4\right)$$

$d \ll \lambda_{\mathrm{th}}$

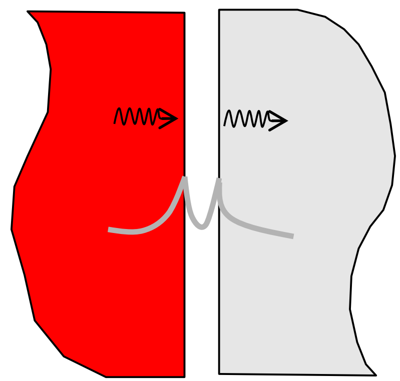

Heat flux exceeds the blackbody limit by orders of magnitude due to tunneling of evanescent waves.

From the point view of wavevector space

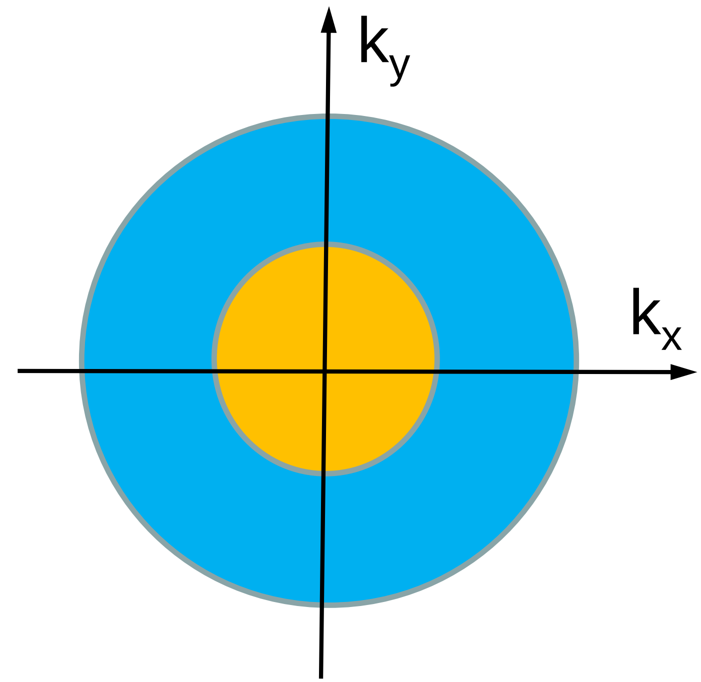

The inner and outer circle denotes propagating and evanescent modes, respectively.

Thermophotovoltaics (TPV)

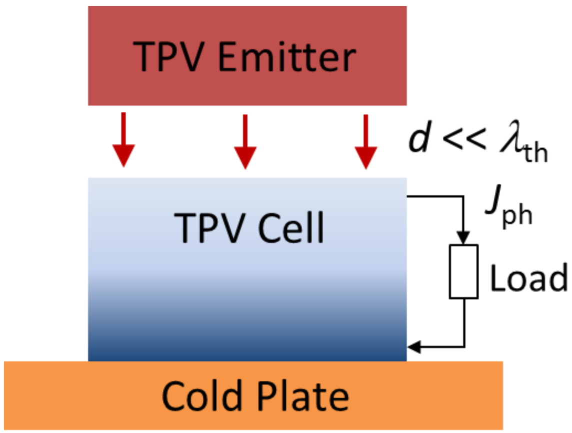

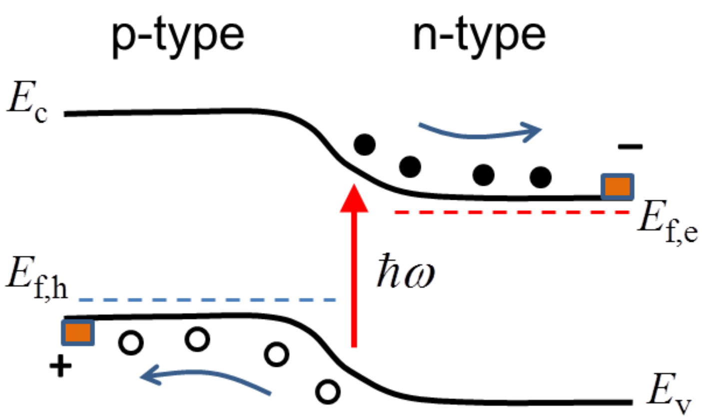

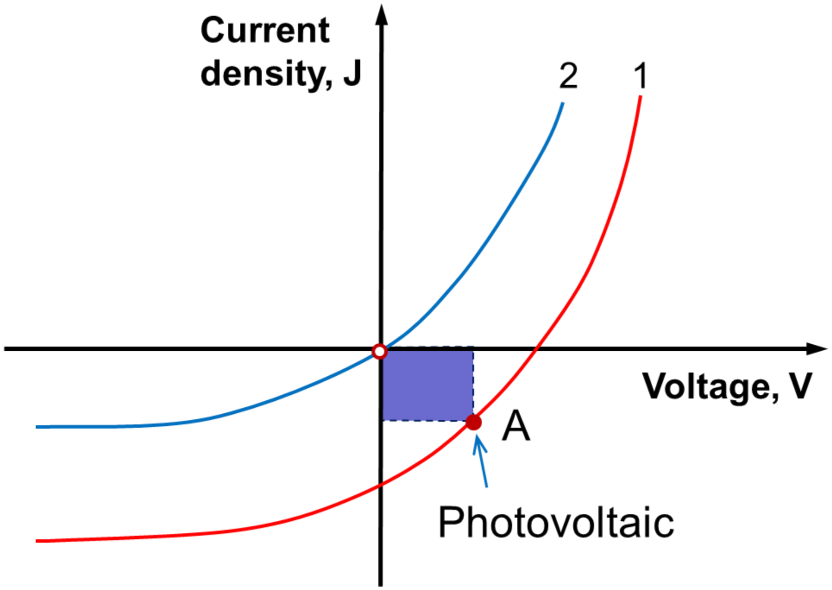

1 PV cell exposed to illumination or a hotter body
2 equilibrium

Near-Field Thermophotovoltaics (TPV)

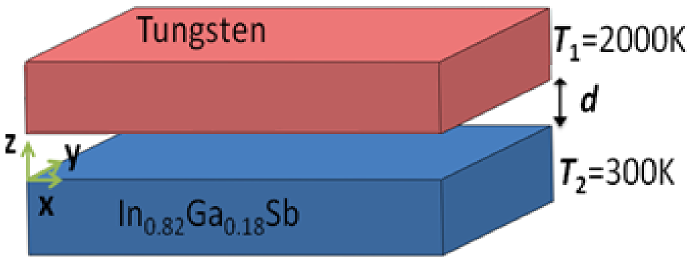

Park et al. JQSRT (2008)

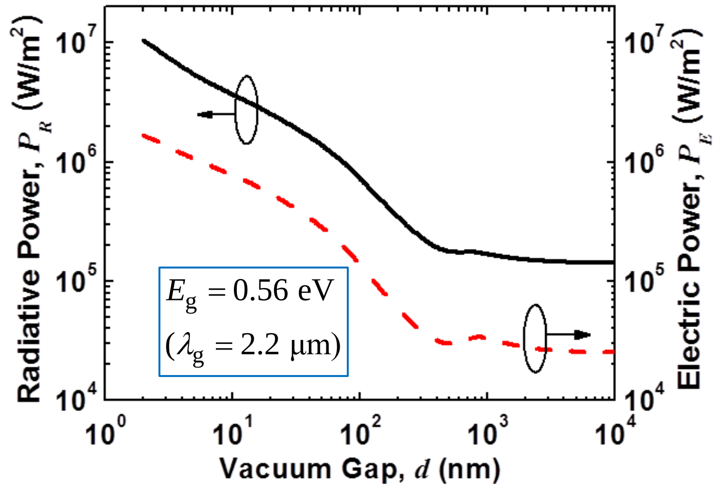

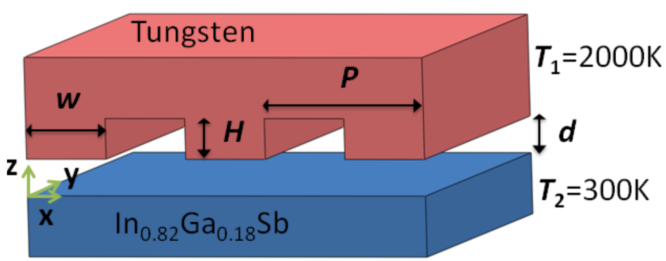

Watjen et al., JHT (2017)

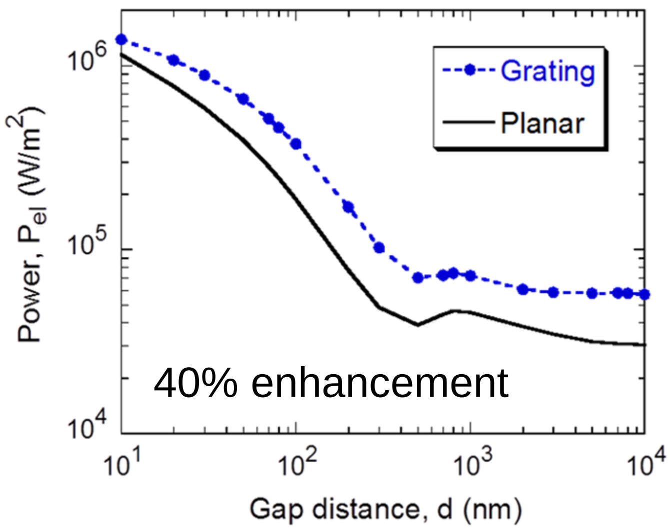

LED and Luminescent Refrigeration

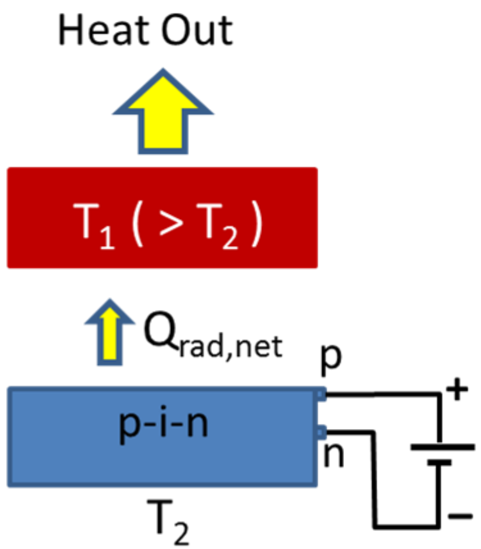

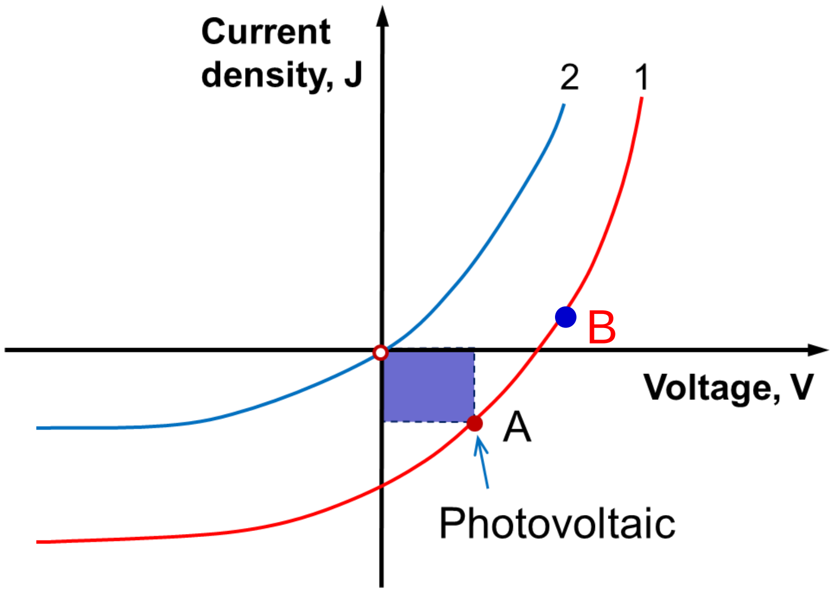

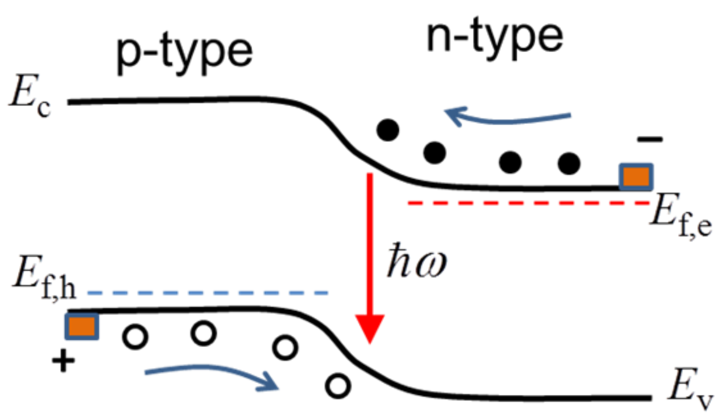

B – electroluminescent effect by providing an active external bias

Can near-field enhance the performance?

Electroluminescent Refrigeration

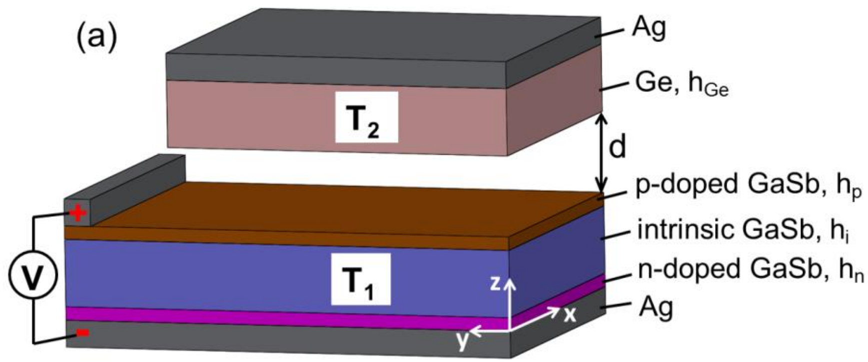

Active region is the intrinsic (i) region.
Backside Ag reflector is modeled as opaque.

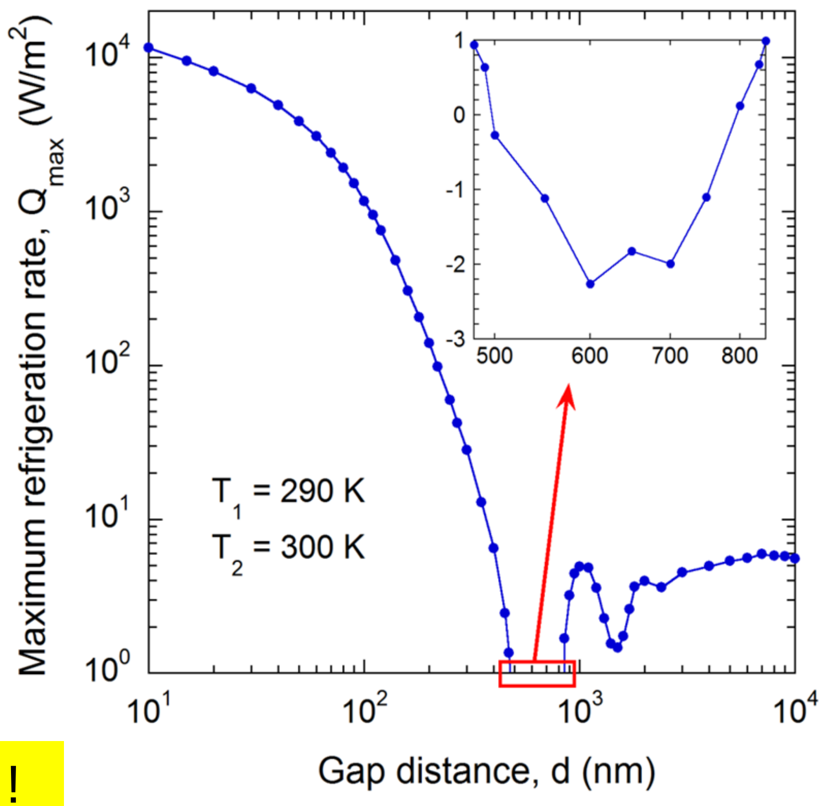

Emit more photons than BB radiation !
Emit even more at nanoscale !!

Liu and Zhang, *Nano Energy* **26** (2016) 353-359.

Planck's Law (1900)

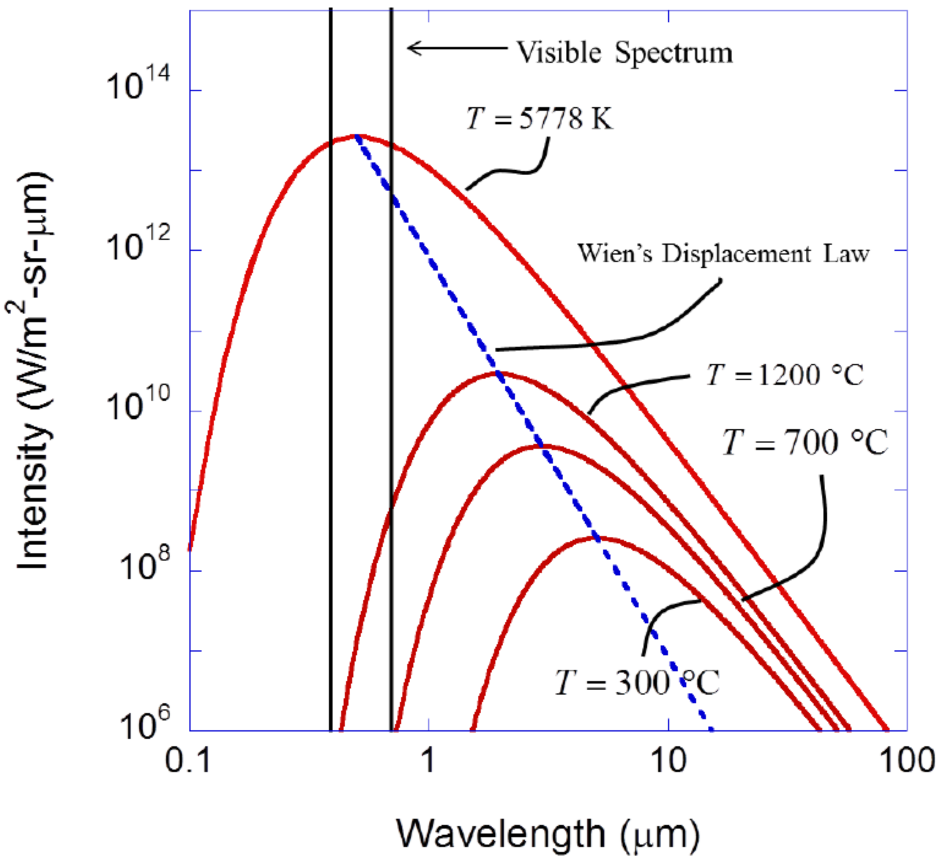

Blackbody emissive power:

$$e_{b,\lambda}(\lambda,T)=\frac{C_1}{\lambda^5(e^{C_2/\lambda T}-1)}$$

Wien's displacement law (1894):

$$\lambda_{\max}\ [\mu\mathrm{m}]=\frac{2898\ [\mu\mathrm{m}\cdot\mathrm{K}]}{T\ [\mathrm{K}]}$$

Characteristic wavelength of thermal radiation:

- 0.5 μm (from the sun)
- 10 μm (from human body)

Photon Chemical Potential Effect

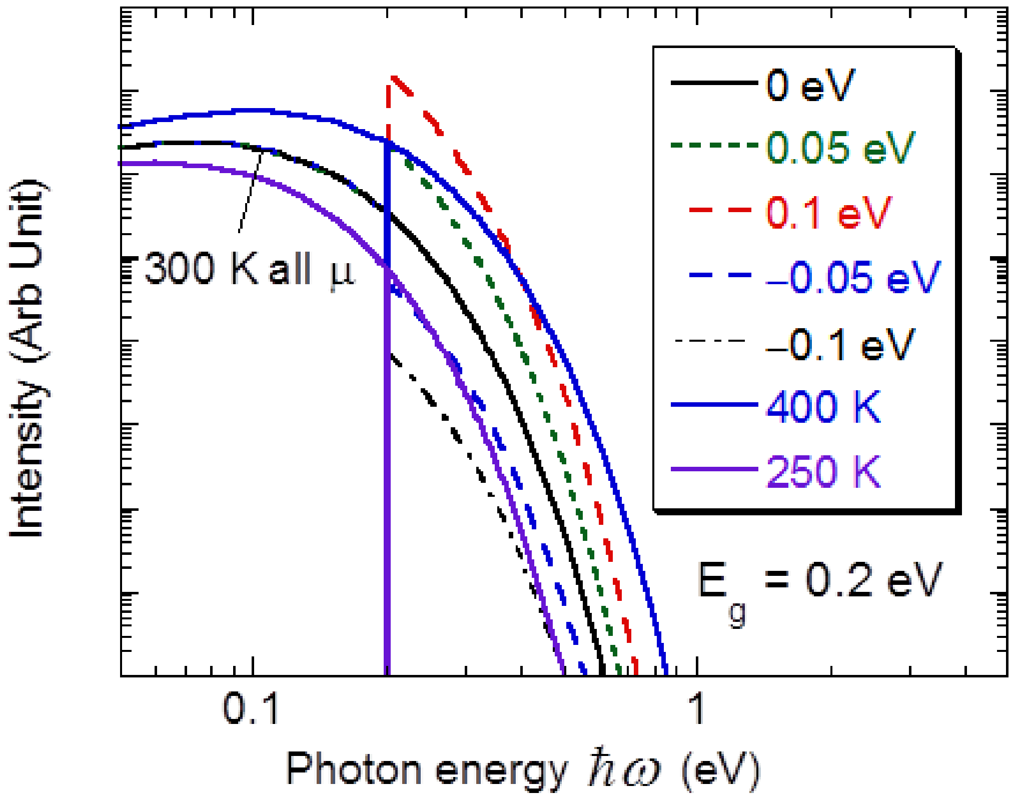

Modified Planck's Law:

$$I(\omega,T,\mu) = \begin{cases} \dfrac{\hbar\omega^3/(4\pi^2c^2)}{e^{(\hbar\omega-\mu)/k_BT}-1}, & \text{for } \hbar\omega > E_g \\ \dfrac{\hbar\omega^3/(4\pi^2c^2)}{e^{\hbar\omega/k_BT}-1}, & \text{for } \hbar\omega < E_g \end{cases}$$

Modified Bose-Einstein Distribution:

$$f_{BE}(\omega,T,\mu) = \frac{1}{e^{(\hbar\omega-\mu)/k_BT}-1}$$

See for example, P. Wurfel, "The Chemical Potential of Radiation," *Journal of Physics C: Solid State Physics* **15,** 3967 (1982).

Photon Entropy

$$f_{\mathrm{BE}}(\omega,T,\mu)=\begin{cases}\dfrac{1}{\mathrm{e}^{(\hbar\omega-\mu)/k_{\mathrm{B}}T}-1}, & \text{for } \hbar\omega>E_{\mathrm{g}}\\[2ex] \dfrac{1}{\mathrm{e}^{\hbar\omega/k_{\mathrm{B}}T}-1}, & \text{for } \hbar\omega<E_{\mathrm{g}}\end{cases}$$

$$\boxed{s_{\omega}(\omega,T,\mu)=k_{\mathrm{B}}\left[(1+f_{\mathrm{BE}})\ln(1+f_{\mathrm{BE}})-f_{\mathrm{BE}}\ln(f_{\mathrm{BE}})\right]}$$

$$\boxed{s(T,\mu)=k_{\mathrm{B}}\int_0^{\infty}s_{\omega}(\omega,T,\mu)D(\omega)d\omega}$$

Non-dimensional entropy content function:

$$\boxed{\psi(\omega,T,\mu)=\frac{Ts_{\omega}(\omega,T,\mu)}{\hbar\omega f_{\mathrm{BE}}(\omega,T,\mu)}}$$

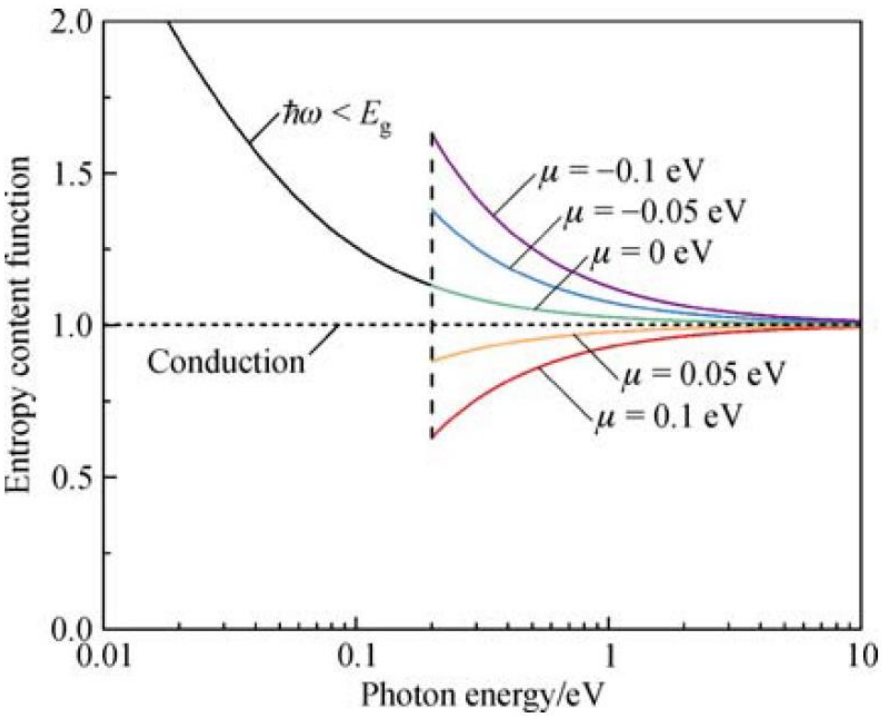

Tervo et al., *Front. Energy* ***12*** (2018) 5-21.
https://link.springer.com/article/10.1007/s11708-017-0517-z

Different Modes of Operation

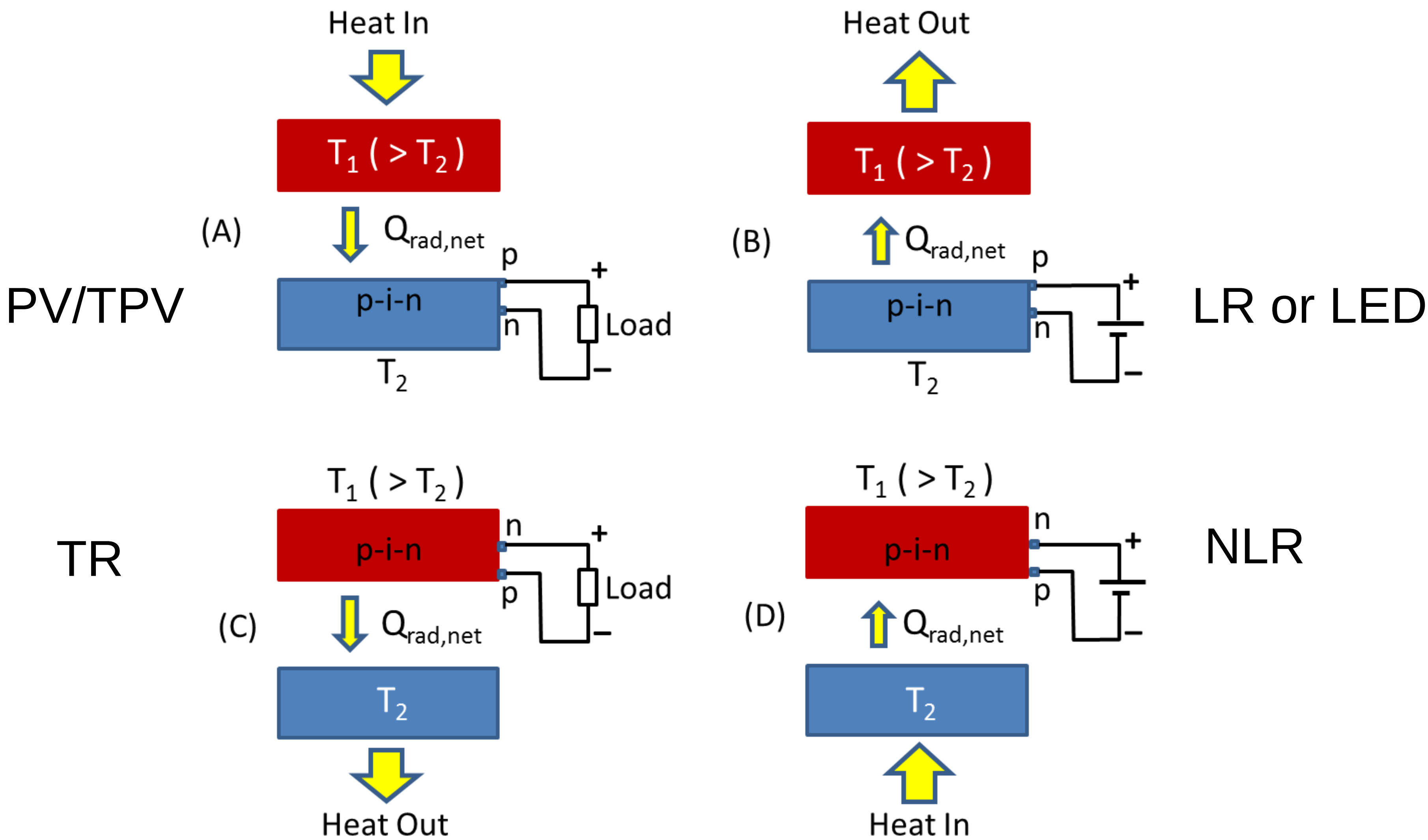

Band Diagrams

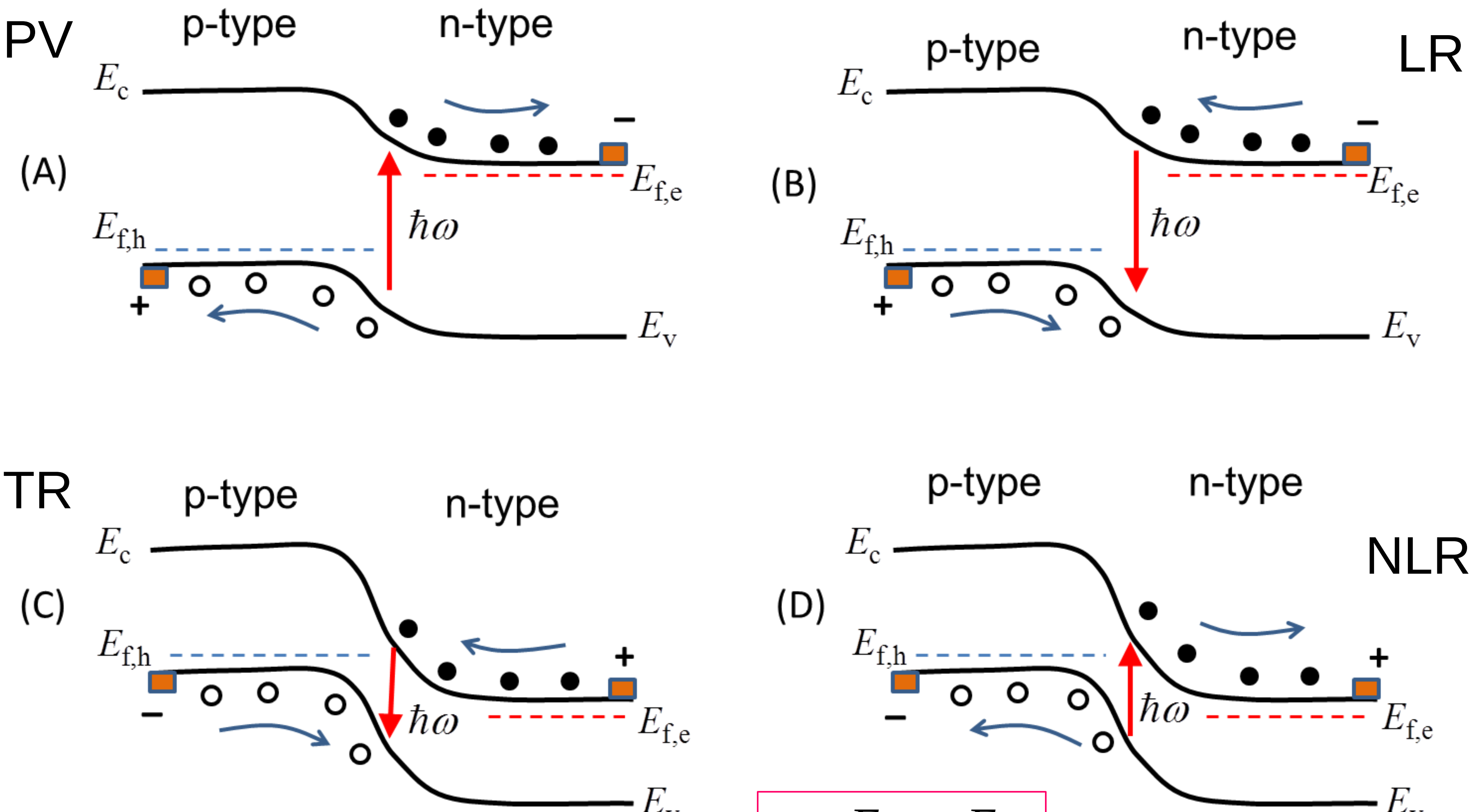

$\mu = E_{f,e} - E_{f,h}$

The J-V Curves

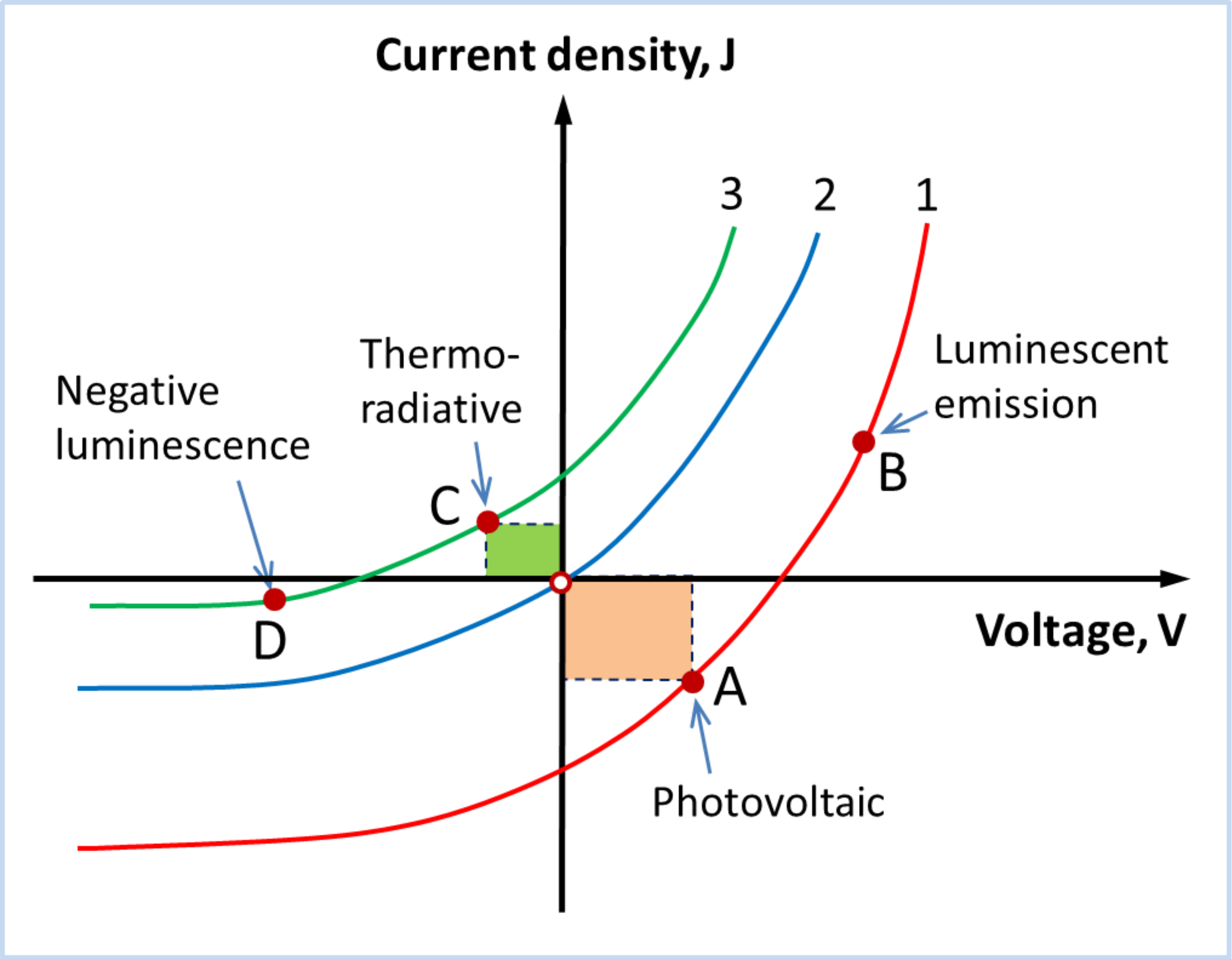

Photon Chemical Potential in Semiconductor p-n Junctions

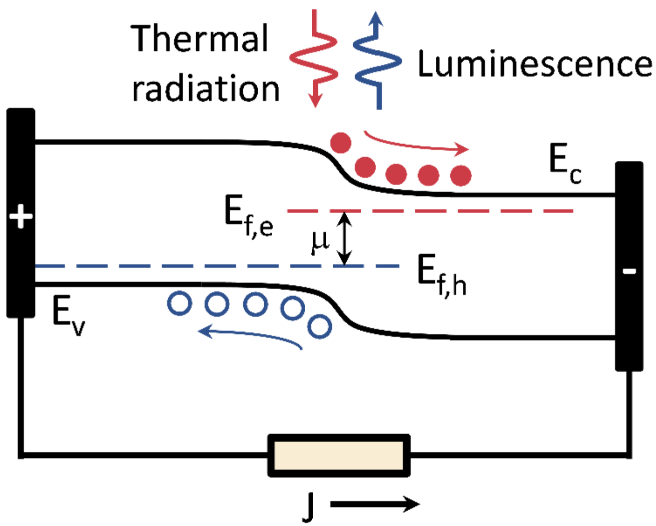

Band diagram for an InAs (E_g = 0.354 eV) cell at 300 K

$$\mu = E_{\mathrm{f,e}} - E_{\mathrm{f,h}}$$

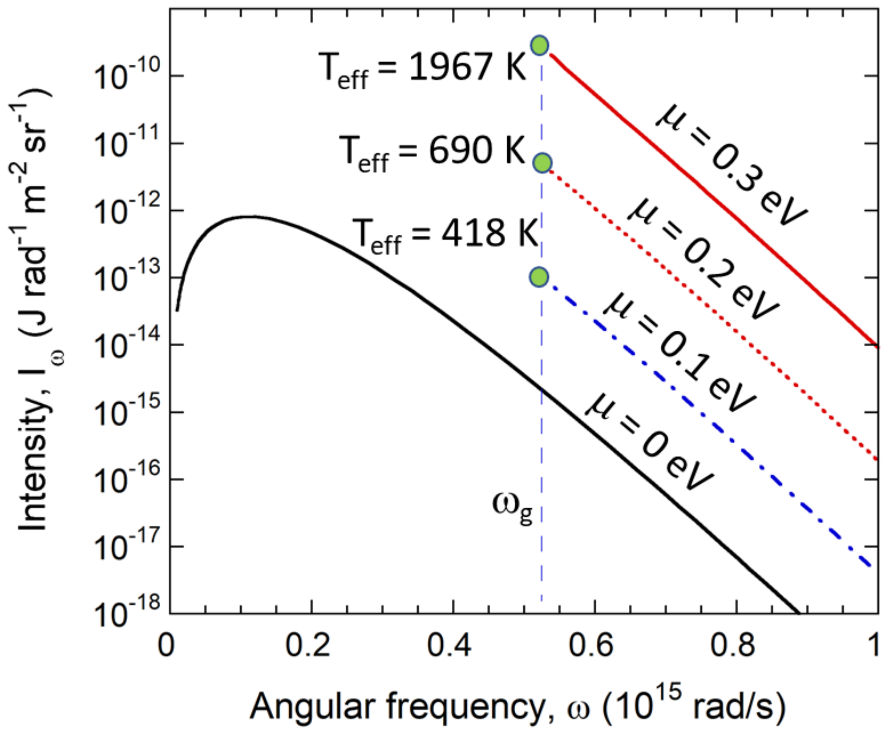

The luminescent emission intensity is a function of the photon chemical potential (μ).

Profile of Photon Chemical Potential

Local concentration of electrons (*n*) and holes (*p*)

$$n = n_{\mathrm{i}} \exp\left(\frac{E_{\mathrm{f,e}} - E_{\mathrm{i}}}{k_{\mathrm{B}} T}\right) \quad \text{and} \quad p = n_{\mathrm{i}} \exp\left(\frac{E_{\mathrm{i}} - E_{\mathrm{f,h}}}{k_{\mathrm{B}} T}\right)$$

Photon chemical potential:

$$\mu(z) = E_{\mathrm{f,e}}(z) - E_{\mathrm{f,h}}(z) = k_{\mathrm{B}} T \ln\left(\frac{n(z)\,p(z)}{n_i^2(T)}\right)$$

It is the difference between quasi-Fermi levels of electrons and holes. Need to model charge transport as well as generation and recombination processes.

Predicted Band Diagrams

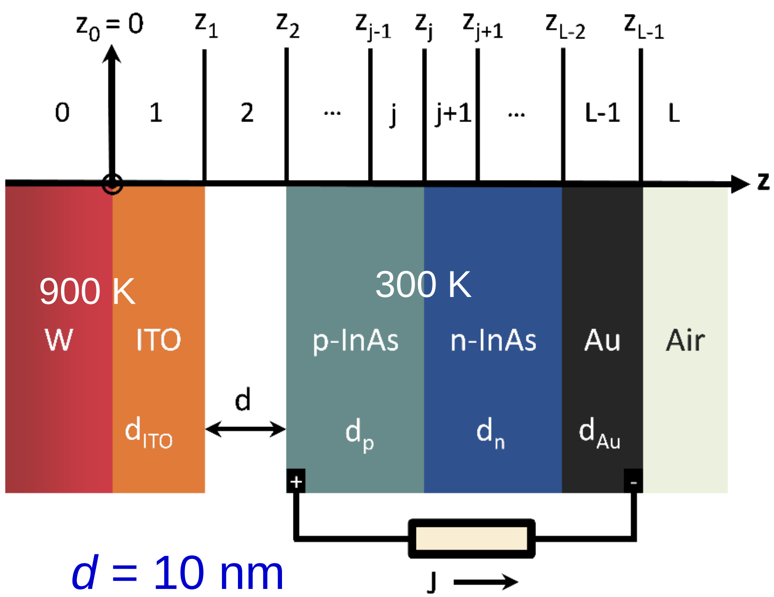

d = 10 nm

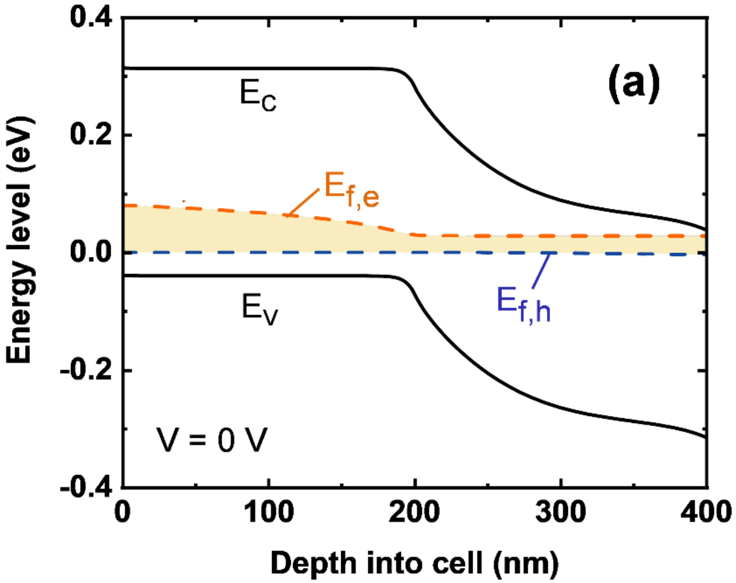

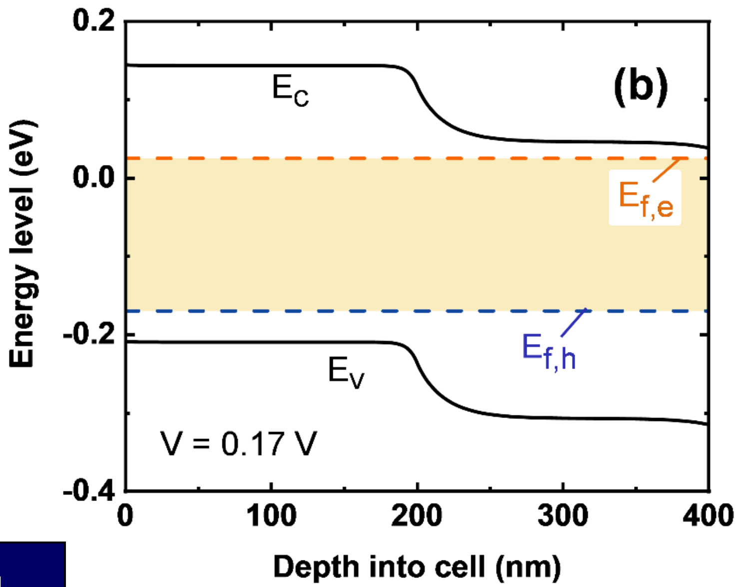

InAs cell is modeled using an iterative method that solves the coupled photon and charge transport problem. Clearly, the photon chemical potential cannot be treated as a constant. Even though the variation of the photon chemical potential may be small, we found that $\mu \neq qV$.

Calculated Photon Chemical Potential

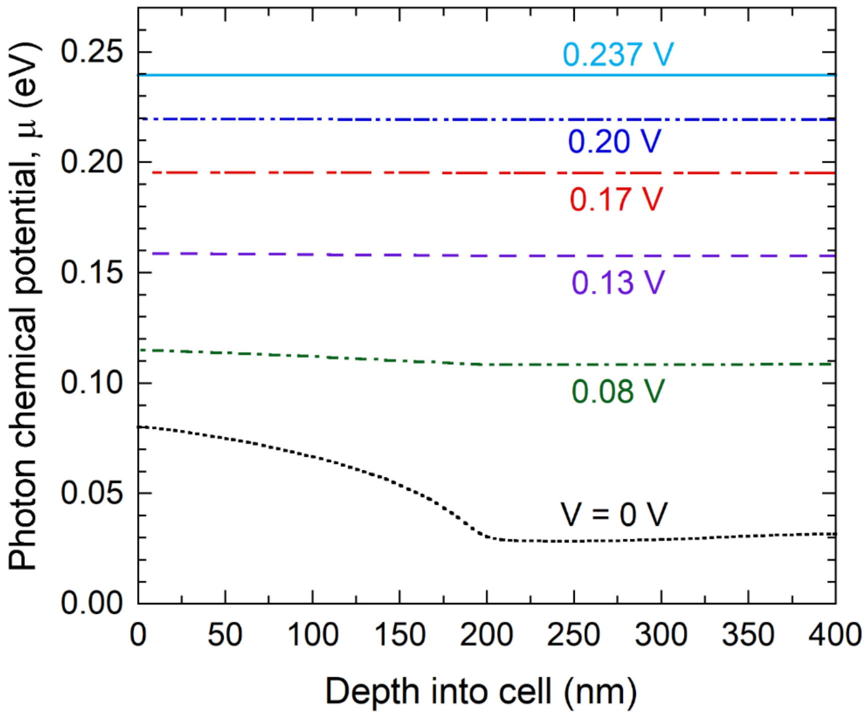

400-nm-thick InAs cell

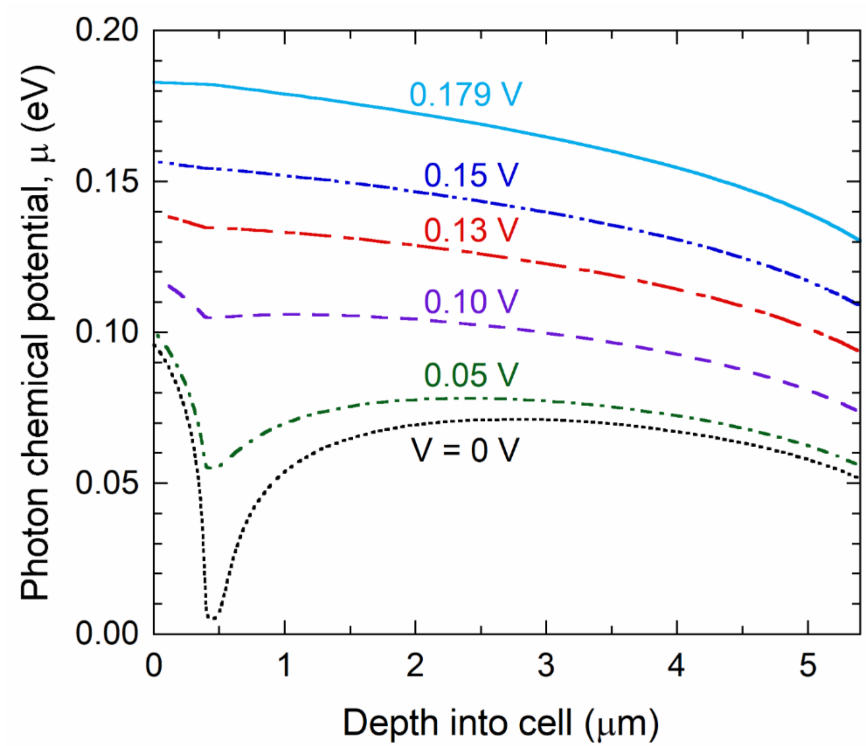

5-μm-thick InAs cell

Take away points: (i) $\mu \neq qV$ (ii) $\mu = f(z)$

Comparison of the TPV Characteristics

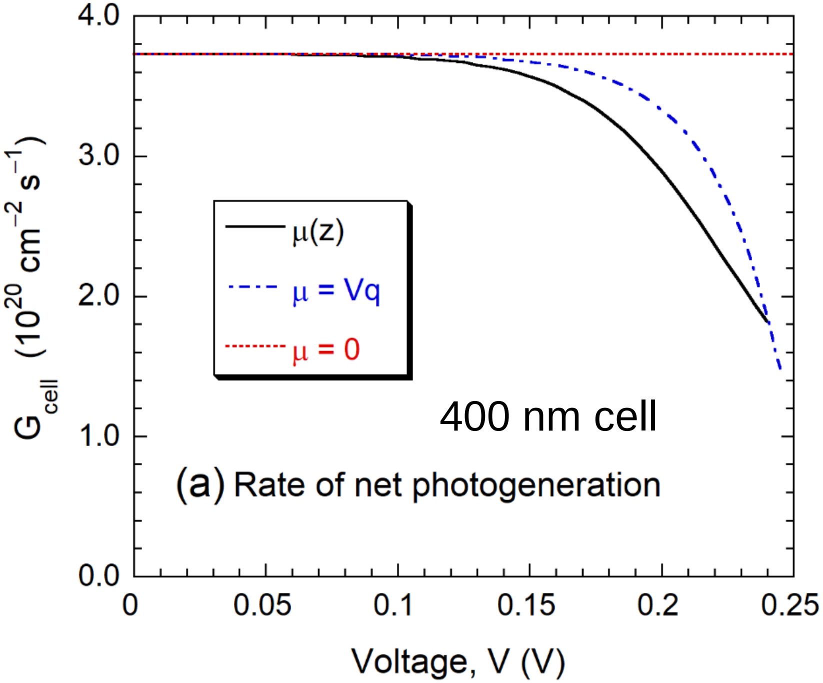

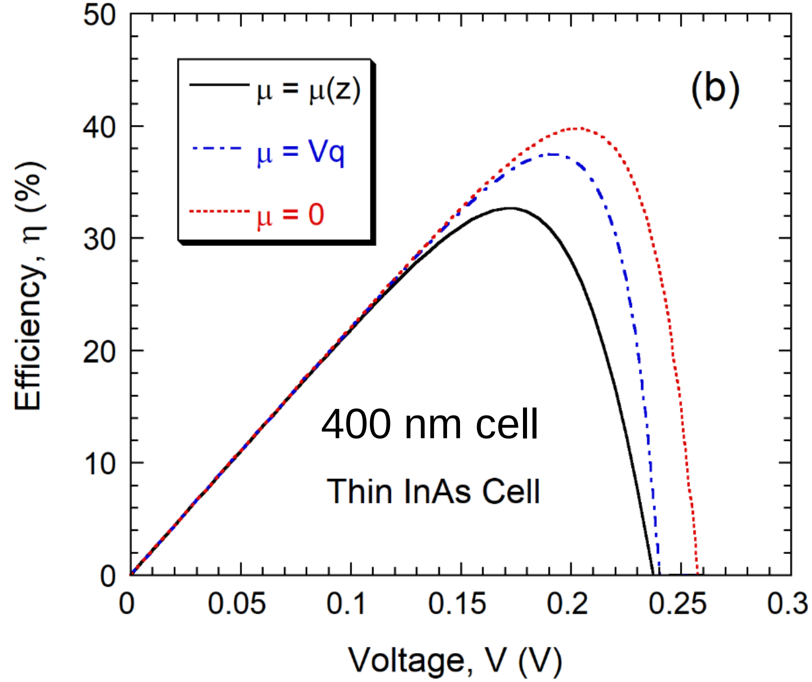

Case (i): $\mu = \mu(z)$ according to the coupled iterative solver considering the photon chemical potential profile.
Case (ii): $\mu = qV$ according to detailed balance analysis considering luminescence effect.
Case (iii): $\mu = 0$ according to detailed balance analysis by ignoring the luminescence effect.

Significant errors may arise by using the detailed balance analysis!

Feng et al., *J. Appl. Phys.* **129** (2021) 213101.

Thermal vs. Nonthermal Radiation

A thermoradiative Cell (TR) with heavily doped InAs cell.

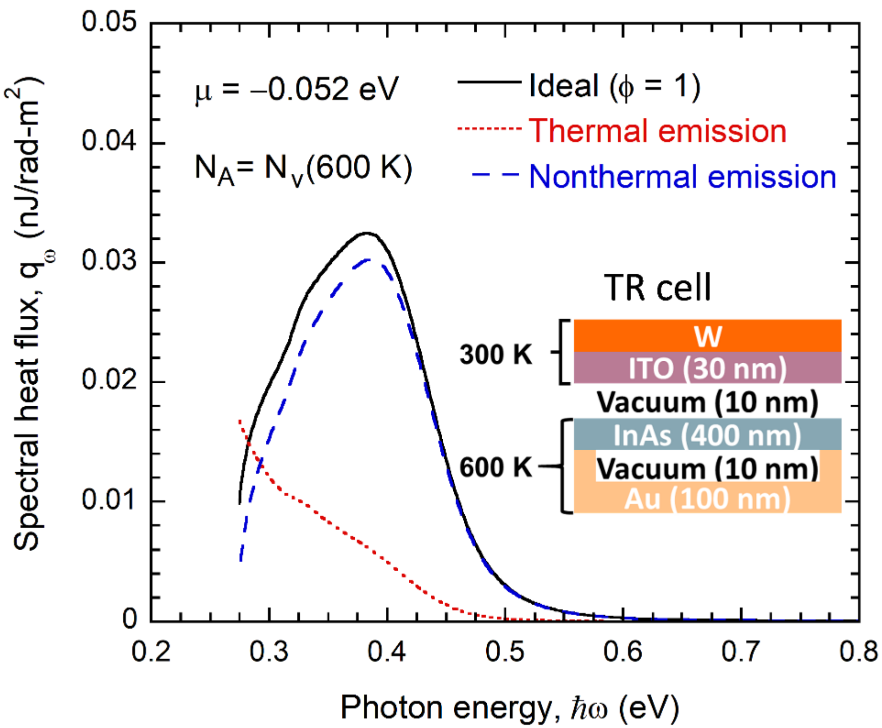

Submitted (2022).

Nonthermal radiation:

$$\sim \varepsilon''_{\mathrm{ib}}(\omega)\Psi(\omega,T,\mu)$$

Thermal radiation:

$$\sim \left[\varepsilon''(\omega)-\varepsilon''_{\mathrm{ib}}(\omega)\right]\Theta(\omega,T)$$

Below bandgap: Only thermal
Above bandgap: There exist a portion of luminescent emission and a portion of thermal radiation

Can Near-Field Radiation Affect the Dark Current?

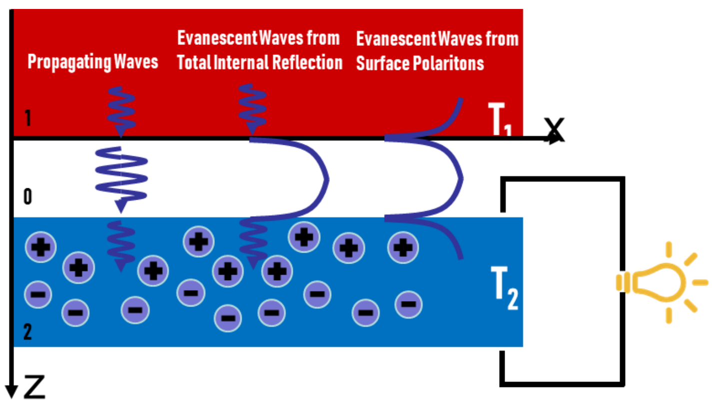

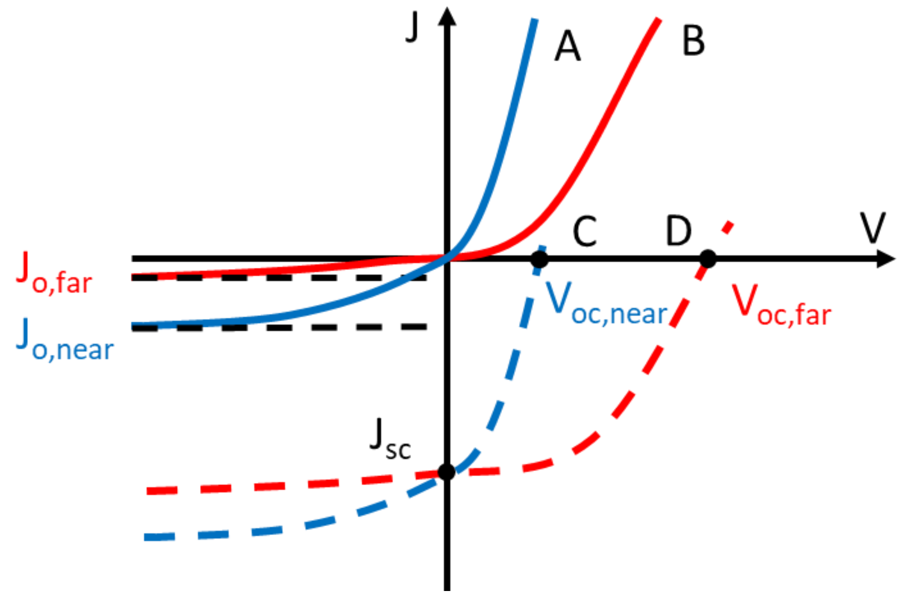

- Curve A is the far-field dark current, Jo is reverse saturation current
- Curve B is the near-field dark current.
- If we simply shift them by adding Jsc (short-circuit current), we will end up with different J-V curves!
- This could impact the analysis of near-field radiative energy conversion devices

Near-Field Effect on (Reverse) Saturation Current

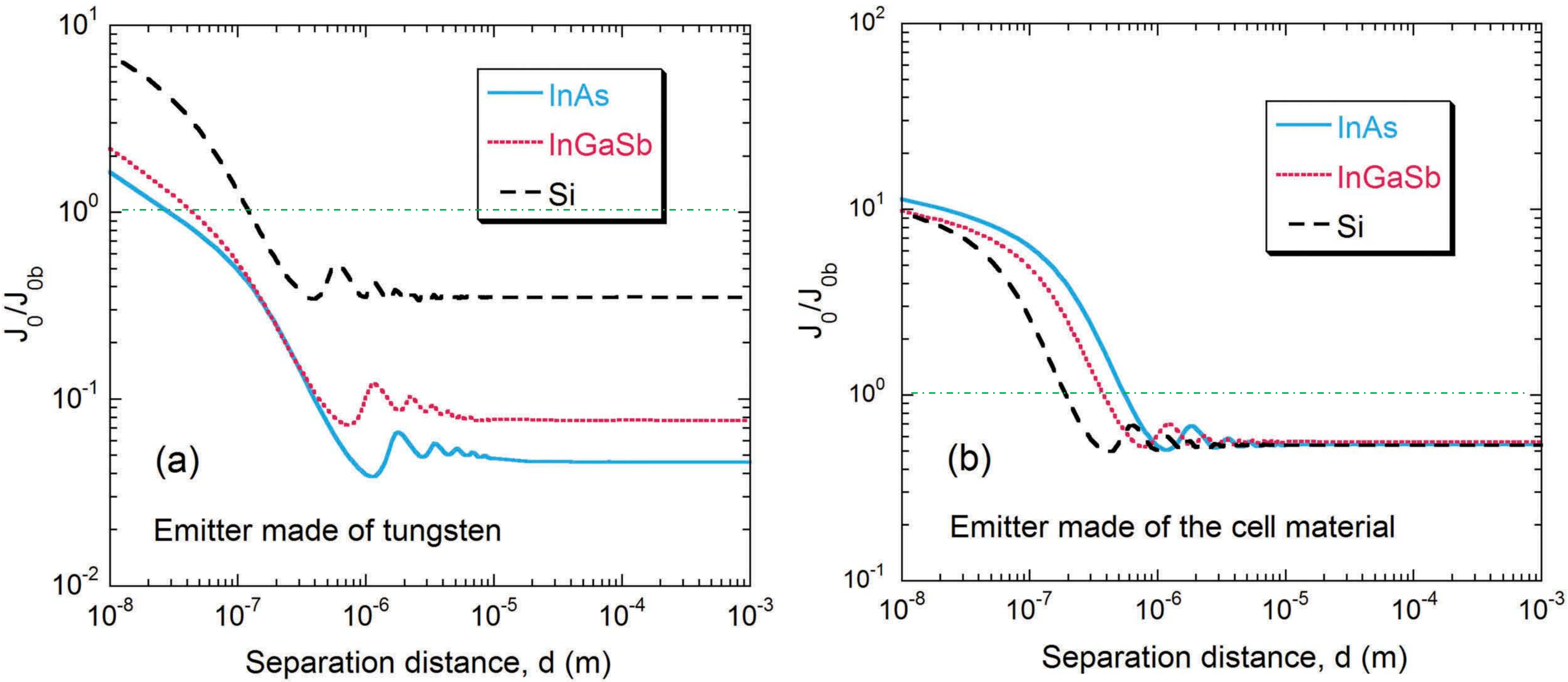

Feng et al. NMTE (2020)

https://doi.org/10.1080/15567265.2019.1683106

Summary

- Near-field operation of thermal radiative energy converters may enhance throughput for power generation and refrigeration.
- The photon chemical potential is an important parameter in near-field semiconductor radiative (or photonic) energy converters and need to be carefully considered when the emitter is at a moderate temperature.
- The accurate modeling of the spatial profile of photon chemical potential provides researchers with a better understanding of photon-charge interactions in semiconductor *p*-*n* junctions.
- Several groups have already demonstrated near-field TPV and LR devices experimentally, though the performance is still relatively low as compared to theoretical predictions.

Future Research Questions

- Can we combine the thermal radiative energy conversion devices to design optimized systems for energy harvesting?
- Can we experimentally validate the photon chemical potential and the modified Planck's law?
- Do we really understand the thermodynamics of semiconductor devices considering photon chemical potential in the near-field regime (*e.g.*, photon entropy and local density of states)?
- How to characterize the polarization status of thermal emission if there are circularly polarization and with nonreciprocal materials?

Acknowledgements

- Department of Energy (DoE)
- National Science Foundation (NSF)
- Current and former students, post-docs, visiting scholars, and collaborators

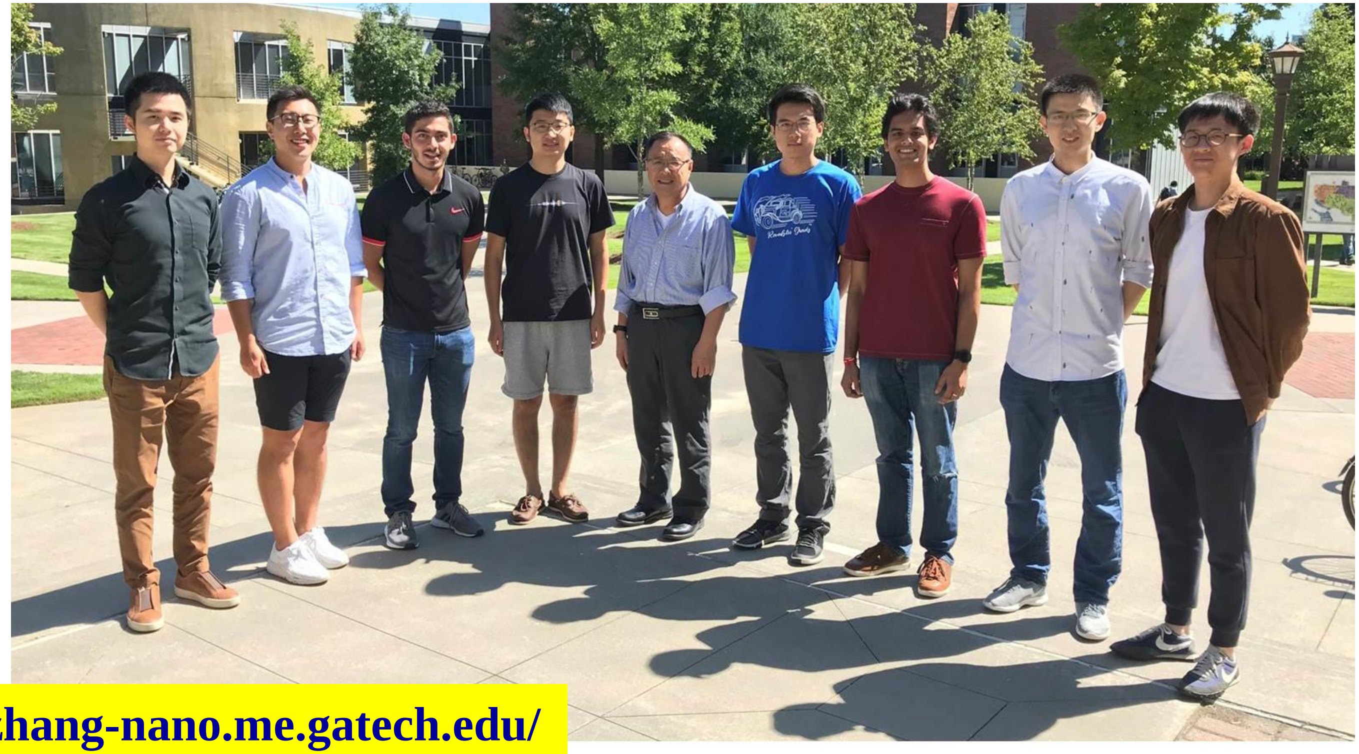

http://zhang-nano.me.gatech.edu/